ON-LINE POWER MONITORING IN CANDU USING PMFD

J. PITRE AND P.S.W. CHAN

Reactor Core Physics Branch
Atomic Energy of Canada Limited
Sheridan Science and Technology Park,
Mississauga, Ontario
Canada
L5K 1B2

1. INTRODUCTION

The use of digital computers in the on-line control of the spatial power distribution has been well established in CANDU reactors [1]. The instantaneous spatial power distribution in a CANDU reactor is calculated on-line, once every 2 min, by the Flux Mapping program. This program synthesizes the global reactor power distribution using a least-squares fit to a set of measured flux detector readings to find amplitudes for a subsequent expansion of a precalculated set of flux harmonics. The reactor control program compares the mapped power shape with the reference power shape. The difference between these two power shapes is minimized by the appropriate deployment of the zone control system.

To minimize computing time and memory requirements, some simplistic assumptions have been built into the Flux Mapping program. Among them are

1. Burnup independent flux to power conversion factor,
2. Smooth harmonic flux shapes calculated from the time-average model, and
3. Individual channel and bundle power ripple caused by refuelling not considered.

These assumptions enable the Flux Mapping program to produce a fairly accurate global power shape within a reasonable time using very modest computing resources. However, it also means that Flux Mapping cannot calculate accurately the maximum channel power and the maximum bundle power in an instantaneous core with refuelling ripple.

In recent years, there has been significant interest in using Slightly Enriched Uranium (SEU) in CANDU reactors. These SEU reactors, which use fuel enrichment up to 3.2 wt % U–235 in the HAC-640 (Highly Advanced CANDU, 640 Channel) core, give significantly higher fuel burnup and greater power uprating potential than the natural-uranium reactors [2].

The higher fissile content and the higher fuel burnup of SEU reactors can result in higher power ripples than those in the CANDU natural-uranium reactors. Also, concerns of fuel performance at high burnup require accurate on-line monitoring of individual rippled channel and bundle powers. The present Flux Mapping program cannot meet the requirements of HAC reactors.

The power mapping finite difference (PMFD) program [3] is specifically designed to supplement or replace the Flux Mapping program in the spatial control system of CANDU SEU reactors. It solves the system of three-dimensional, two-energy-group neutron diffusion equations on-line. A unique feature of PMFD is its ability to use measured detector fluxes as internal boundary conditions in the flux solution. The resulting flux shape satisfies both the distribution of material properties and the measured flux values.

The PMFD model is very similar to the model used in a conventional off-line fuel management program such as RFSP [4]. The present PMFD model for the HAC-640 core includes 640 fuel channels and 224 reflector mesh points in the radial plane. There are 24 axial meshes. Each axial mesh, which is one-half a fuel-bundle in length, has a unique set of lattice properties according to the type of fuel bundle, current irradiation and presence of reactivity devices. The PMFD program can be initialized at any instant by downloading the appropriate fuel irradiation distribution from any off-line fuel management program. Beginning from this point, PMFD will update the fuel burnup distribution in the core continuously, according to the reactor power history and the refuelling schedule. The power distribution in the core at any time can be calculated on demand, always using the most up-to-date information.

2. METHODOLOGY, VALIDATION AND EXECUTION SPEED

2.1 Methodology

The execution of the PMFD program is illustrated in Figure 1. Initially, the DIFFUSION module calculates the reactor flux and power distributions on the basis of diffusion theory alone, along with lattice properties and the current configuration of the reactivity devices. From the flux distribution, the module INTERP then calculates a set of simulated readings at the locations of the flux-mapping detectors, using a quadratic interpolation method. The simulated detector readings are then compared against the measured detector readings. A user-definable algorithm may be used to rationalize the discrepancies between simulated and measured detector readings. (For example, discrepancies greater than 10% result in simulated detector readings being used.) Each rationalized detector reading, which can be a simulated or a measured reading, or a user-definable combination of the two, is used to define the flux values at the eight mesh points closest to the detector. This internal boundary definition is accomplished by determining the ratio between the rationalized detector reading and the detector reading as calculated by the diffusion calculation, which is determined by a three-dimensional parabolic interpolation. The flux values at the eight neighbouring mesh points are then adjusted by this ratio. These flux values are used as internal boundary conditions in the MAPPING module, which calculates the final flux and power distributions using diffusion theory.

2.2 Validation

The results calculated by the DIFFUSION module are in good agreement with those calculated by the 3DDT code [5] for the same reactor model. The results calculated by the MAPPING module were validated in this study using RFSP simulation results carried out in a 1000 FPD refuelling simulation of the HAC 640 core. The results indicated that using detector readings as internal boundary conditions significantly improves the accuracy of the flux calculations based on those calculated by diffusion theory alone. Further tests, described here, were performed to show that the PMFD procedure is insensitive to both random and systematic errors in measured detector readings.

2.3 Execution Speed

Various versions of PMFD have been implemented in many different computers, from the IBM PC to the various versions of HP 700 series work stations. The execution of a complete PMFD simulation requires less than 2 min on the HP 700 workstation and less than 5 min on the Intel Pentium series personal computers.

3. APPLICATIONS

The PMFD program can be used in two entirely different modes: simulation and prediction. In the simulation mode, PMFD calculates fluxes and powers in the core on the basis of input information such as channels refuelled, reactor power level, control-device positions, and flux detector readings. In this mode PMFD simulates what has already happened in the reactor. The simulated results can be used to compare with available measurements. Good agreement between simulation and measurements assures the reactor operators that the reactor is performing as expected. However, the additional benefit of implementing PMFD on-line is the ability of PMFD to predict how the reactor will respond to a certain action before that action actually takes place. This prediction is not limited by pre-conceived reactor configurations, but is based on the most current status of the reactor. Moreover, it is available on demand, that is, at the very instant when intelligent information is needed. For example, a reactor operator can consult the PMFD program to determine if it is safe to change the reactor power, to refuel a certain channel, or to raise a certain bank of adjuster rods because of the the current reactor conditions. Some of the potential applications of PMFD are described in the following sections.

3.1 On-line Power Mapping and Spatial Control Detector Calibration

PMFD combines theory and measurements to produce up-to-date flux and power distributions at any instant. The relative powers calculated by PMFD can replace the relative fluxes presently calculated by Flux Mapping for zone control detector calibration purpose. This will significantly improve the accuracy of the spatial control system.

3.2 On-Line Fuel Management Simulation and Prediction

The PMFD program can be executed immediately after a channel is refuelled. Thus channel power ripple and bundle powers in the refuelled channels can be calculated accurately. The present off-line RFSP fuel management program is typically executed by the station physicist once every 2 or 3 d. On the basis of the frequency of execution, an on-line PMFD fuel management simulation is expected to be more accurate than the off-line RFSP simulation. As discussed previously, PMFD can be used to predict the effect of refuelling a certain channel before the refuelling process actually takes place.

3.3 On-Line Selection of Channels for Refuelling

Refuelling is a major cause of power and reactivity perturbations in CANDU reactors. Some of the factors that influence the selection of a particular channel for refuelling are

1. Present channel age (i.e., burnup),
2. Present channel power,
3. Estimated powers of a channel and its neighbouring channels upon refuelling,
4. Estimated effect on reactor overpower protection margin upon refuelling,
5. Present zonal power distribution,
6. Present zone-control fill distribution, and
7. Any other relevant criteria.

The selection of channels for refuelling therefore requires considerable reactor physics knowledge and engineering judgment. The selection process is more difficult in the HAC core than in natural-uranium cores because of the higher perturbation caused by the higher fissile content of the HAC fuel. However, it is possible to build intelligence in the PMFD program such that it will, on demand, select the best channels for refuelling under the current reactor condition. Also, the selections can be confirmed by a pre-simulation to help ensure that the consequences of refuelling these channels are acceptable.

3.4 Load Following Simulation and Prediction

It is sometimes desirable to adjust the power output of a reactor to follow the grid demand. However, the large xenon perturbation that occurs when the reactor is operating in this load-following mode causes extensive perturbations in reactivity and spatial power distribution. The movement of reactivity devices, such as zone controllers, adjuster rods and mechanical control absorbers dramatically change the reactor power shape during the load following operation. The present practice of using the off-line simulations may not provide adequate up-to-date information to the operators. The PMFD program, on the other hand, will follow the reactor power history and reactivity device deployment precisely to give the operators up-to-date power distributions. Also, it is possible to pre-simulate a planned load following operation to ensure that the reactor will be operating within the operating limits under these conditions.

4. PERFORMANCE OF PMFD

If flux detectors are not used as internal boundary conditions, PMFD should give the same results as RFSP, provided that the same mesh structure and the same lattice parameters are used in both programs. In this study, PMFD represents a HAC core using 1 mesh point per channel in the x-y plane and 2 points per bundle in the z plane. The RFSP model has as many as 4 mesh points per bundle, that is 2 mesh points radially and 2 mesh points axially. Thus the present PMFD model is not expected to give the same results as RFSP. This discrepancy is mainly due to the difference in mesh structure and the representation of reactivity devices. The same lattice properties and the same fuel-burnup distribution are used in both programs. The coarse-mesh PMFD model was used in this study in order to demonstrate that

1. The PMFD program can be executed on an inexpensive microcomputer in less than 2 min, and
2. The discrepancy between the coarse mesh PMFD and fine mesh RFSP results can be significantly reduced by using detector readings extracted from RFSP simulations; PMFD accuracy could be increased by a finer mesh as well as by using measured detector readings.

It should be noted that reactivity devices such as adjuster rods and zone controllers are homogenized over a larger volume in the coarse-mesh PMFD model than in RFSP. This over-homogenization weakens the local flux shaping capability of the reactivity devices in the coarse mesh PMFD model. Hence the coarse-mesh PMFD is expected to give slightly higher maximum bundle power and maximum channel power than RFSP. This overestimation can be significantly reduced or eliminated in a fine-mesh PMFD model. However, conservative estimates of maximum bundle power and maximum channel power could be a desirable feature of an on-line power monitoring program.

The effectiveness of the measured detector readings depends on how accurate the theoretical simulation model represents the real reactor and the accuracy of measured detector readings. If the theoretical model is perfect, then using measured detector readings will not improve the accuracy of the simulation. The RFSP and PMFD models, however detailed, will not be perfect because there are always uncertainties in the reactivity-device position measurements, the coolant densities, the fuel temperatures, the lattice parameters and the fuel burnup distribution used in the simulations. Because the detector readings are measured in the real reactor environment, incorporation of these measurements should improve the representation of the real reactor core in the simulation model and therefore should improve the simulation accuracy.

4.1 Assessment of PMFD Accuracy

The accuracy of the present coarse–mesh PMFD HAC model was evaluated by comparing the PMFD power distributions with the corresponding RFSP power distributions for three instantaneous cases: FPD 60, FPD 540 and FPD 1000 in the HAC 640 refuelling study, performed with RFSP. In each case, the comparisons were carried out for the following conditions :

1. PMFD diffusion calculation only
2. PMFD mapping calculation with no random detector errors, and
3. PMFD mapping calculation with 5% Gaussian random detector errors.

The detector readings were taken from the RFSP simulations and were assumed to have no error. Each set of comparisons was carried out for three different reactivity-device configurations,

1. Nominal, i.e. all adjusters inserted, nominal zone controller fills
2. All zones drained, all adjuster rods inserted, and
3. Nominal zone controller fills, all adjuster rods withdrawn out of core.

The results of these comparisons are summarized in Tables 1 to 3. The discrepancies between PMFD diffusion calculations and RFSP diffusion calculations for nominal reactivity device configuration are between 2.7% to 3.7% rms over the whole core for channel power. Using flux detector readings extracted from RFSP simulations reduces the discrepancies to about 1.5% root mean square for channel power. This represents an improvement of about 50% in the PMFD channel power mapping accuracy. There are also significant improvements in the agreement between PMFD and RFSP calculated maximum channel powers for most cases. The discrepancy between PMFD and RFSP results is defined as (PMFD–RFSP)/RFSP in this study.

Adding 5% Gaussian random errors to the RFSP simulated detector readings produces a degradation of less than 0.5% rms in channel-power mapping accuracy. The degradation of the PMFD mapped maximum channel power and maximum bundle power is about 1% and 1.5% respectively. Therefore, random errors of this magnitude in detector signals do not introduce significant local errors in the PMFD mapping procedure.

Figures 2 to 4 show the channel power discrepancy between PMFD and RFSP calculations at FPD 1000. In these figures, any difference of less than 0.1% is left intentionally blank. The PMFD and RFSP channel powers in row M, the reactor midplane, are shown in Figure 5. The PMFD and RFSP bundle powers in a central channel, M-14, are shown in Figure 6.

These results demonstrate that the discrepancies between PMFD and RFSP can be significantly reduced by using RFSP calculated detector readings in PMFD. The degradation in PMFD mapping accuracy caused by random error is relatively small compared with the improvements achieved by using the detector readings. There is no evidence that random detector errors introduce significant local distortions in the PMFD mapping results. Perturbations caused by to zone controller draining or adjuster rod withdrawal have negligible effects on the accuracy of the PMFD calculations.

The FPD 1000 case was used to carry out additional detailed assessments of PMFD accuracy for the following conditions:

1. Ten unique sets of random detector error distributions,
2. Systematic error caused by the loss of signal from one central and one peripheral detector assembly, and
3. Random errors in lattice cross sections caused by uncertainties in fuel burnup and nuclear data.

4.2 Random Detector Errors

The output from a flux-mapping detector in an operating reactor consists of both true neutronic signal and random noises which vary from one detector to the next. The effect of the noise component at any particular detector at any particular time is a random phenomenon. It can either increase or decrease the output of a detector with respect to the true neutronic signal. The random error component of the detector signal is completely unpredictable and cannot be filtered out. However, the effect of random detector error on the power-mapping accuracy of either Flux Mapping or PMFD can be simulated by multiplying the measured detector readings by a random error factor. The distribution of the random error factors in each set is a normalized Gaussian distribution with a specified standard deviation, typically 5% in flux-mapping analyses. Each set of random error factors consists of 119 numbers, corresponding to each of the 119 flux detectors. It is necessary to carry out the power-mapping procedure with several sets of random factors in order to evaluate the random error effect on a statistical basis.

The effect of random detector errors on PMFD mapping accuracy was evaluated for the FPD 1000 case with 10 sets of random detector error factors, which have a mean of 1.00 and a normalized standard deviation of 0.05. The PMFD simulations were repeated using detector readings extracted from the RFSP 1000 FPD simulation and then multiplied by the error factors. The results are summarized in Table 4. The average degradation in PMFD mapping accuracy is about 0.5% rms for channel power, 0.9% for maximum channel power and about 1.6% for maximum bundle power. Hence random detector errors do not produce significant global or local mapping error.

4.3 Systematic Errors

There are two major sources of systematic errors:

1. Some detectors may consistently give higher or lower readings than the true flux levels.
2. All detectors in the same flux detector assembly may fail simultaneously.

Because PMFD calculations can be carried out independently of the flux detectors (in the DIFFUSION module), they can be used to detect any systematic errors, which are mainly due to incorrect calibration of the detectors. A set of theoretical detector readings can be produced by PMFD at any instant based on diffusion theory without using detector readings. These theoretical readings can be compared with the corresponding measurements. Several such comparisons over a reasonable time period will establish a pattern that will expose systematic errors. These systematic errors can be eliminated by calibrating the suspected in-core flux detectors with a "Travelling Flux Detector", which has been specifically developed by AECL for this purpose.

The current Flux Mapping program in the CANDU-6 natural-uranium reactors depends exclusively on the flux detector readings to synthesize the reactor flux distribution from a pre-calculated set of harmonic mode fluxes. The locations of the flux detectors have been carefully chosen to provide accurate prediction of the flux shapes under various expected reactor configurations. The failure of a significant number of detectors, especially if they are concentrated in one location, for example, in the same flux detector rod assembly, may skew the calculation of modal amplitudes. This kind of systematic error could significantly affect the accuracy of the Flux Mapping program. The PMFD program, on the other hand, generates most of the information through the diffusion calculation, which depends mainly on the fuel irradiation and reactivity device configuration only. Whereas detector signals are crucial in Flux Mapping, they are additional constraints in PMFD. Therefore PMFD is not expected to be sensitive to the systematic loss of detector signals.

Four simulations were carried out to assess PMFD sensitivity to the loss of detector signals:

1. The loss of a corner flux detector assembly, that is, VFD-24, which has 5 detectors, and
2. The loss of a central flux detector assembly, that is, VFD-8, which has 7 detectors

These flux distributions were compared with the flux distributions calculated for no loss of detectors and that for the loss of all detectors (the diffusion solution alone). The results of the above analysis are summarized in Table 5. As expected, the degradation in PMFD accuracy caused by the loss of a few detector signals is minimal, that is, less than 0.1% difference in rms error for channel power. However, the use of detector signals does improve the PMFD accuracy significantly.

4.4 Lattice Parameter Error

The accuracy of any neutronic diffusion code, such as RFSP and PMFD, depends on the accuracy of the lattice parameters, for example, absorption and fission cross sections, used in the simulations. There are always uncertainties in these lattice parameters because the concentrations of the uranium, plutonium and other isotopes in each fuel bundle in the core cannot be calculated with absolute accuracy. The flux detectors, however, measure the flux distribution of the operating reactor, including the effects of elements that cannot be represented in the theoretical model. Thus measured detector readings provide very useful additional information to the theoretical model.

The effects of lattice cross-section error on PMFD accuracy were evaluated by applying a Gaussian random error distribution (standard deviation 1%) to the fuel-burnup distribution obtained from the RFSP 1000 FPD simulation. The random deviations in burnup generates random deviations in the burnup-dependant lattice cross sections used in PMFD calculations. Three unique sets of random errors were used in the PMFD diffusion and PMFD mapping calculations. The mapping calculations include the combined effects caused by lattice cross-section errors and random detector errors.

Table 6 summarizes the results of the analysis. The error caused by the uncertainty in lattice parameters is 2.6% rms for channel power for the diffusion calculations. This is reduced to 1.44% rms using the PMFD mapping procedure. These results indicate that using detector readings obtained from an operating reactor should improve the accuracy of the diffusion calculations.

5. CONCLUSIONS

The PMFD program has been shown to be an accurate method of monitoring channel and bundle powers on-line in CANDU reactors. Also, PMFD results have been found to have low sensitivity to random and systematic errors in flux-detector measurements. Consistency between PMFD and conventional diffusion calculations can be further improved by adding more meshes to the PMFD model. Computers that are fast enough to solve a detailed PMFD model on-line within two minutes, are readily available today at moderate prices.

ACKNOWLEDGEMENT

The authors are grateful to EPDC for the financial support for this work and for the permission to publish this paper.

REFERENCES

1. E. Hinchley and G. Kugler, "On-Line Control of CANDU-PHW Power Distribution", AECL-5045, March 1975.

2. P.S.W. Chan and A.R. Dastur, "The Role of Enriched Fuel in CANDU Power Uprating", Proceedings of the 8th Annual Conference, Canadian Nuclear Society, Saint John, New Brunswick, June 1987.

3. P.S.W. Chan and M. Mamourian, "Application of On-Line Solution of 3-Dimensional Multigroup Finite-Difference Neutron Diffusion Equations in Reactor Power Control System", Third International Conference on Simulation Methods in Nuclear Engineering, April 18-20, 1990, Montreal, Quebec.

4. B. Rouben, "Overview of Current RFSP-Code Capabilities for CANDU Core Analysis", AECL-11407, January 1996.

5. John C. Vigil, "3DDT, A Three-Dimensional Multigroup Diffusion-Burnup Program", LA-4396, Los Alamos Scientific Laboratory of the University of California, Los Alamos, California, February 1970.

Table 1 Assessment of PMFD Accuracy Using RFSP Data at FPD 60

Case			RFSP simulations		PMFD simulations		
zones	adjusters	type	Maximum Channel (kW)	Maximum Bundle (kW)	Maximum Channel (kW)	Maximum Bundle (kW)	Channel Power RMS Error
nominal	in	diff	7357	954	7465	1096	3.45
nominal	in	map			7521	999	1.47
nominal	in	err			7527	1012	1.82
empty	in	diff	9078	1213	9138	1268	2.52
empty	in	map			9144	1258	1.28
empty	in	err			9196	1275	1.52
nominal	out	diff	9612	1375	9560	1410	2.96
nominal	out	map			9514	1395	1.35
nominal	out	err			9659	1378	1.77

Table 2 Assessment of PMFD Accuracy Using RFSP Data at FPD 540

Case			RFSP simulations		PMFD simulations		
zones	adjusters	type	Maximum Channel (kW)	Maximum Bundle (kW)	Maximum Channel (kW)	Maximum Bundle (kW)	Channel Power RMS Error
nominal	in	diff	7229	968	7592	1024	3.70
nominal	in	map			7257	992	1.36
nominal	in	err			7341	1000	1.79
empty	in	diff	9144	1296	9209	1350	2.07
empty	in	map			9269	1329	1.22
empty	in	err			9284	1349	1.50
nominal	out	diff	9521	1332	9622	1407	2.98
nominal	out	map			9547	1386	1.25
nominal	out	err			9603	1373	1.74

note:
diff = Diffusion theory Only
map = Diffusion + mapping (no detector errors)
err = Map with 5% Gaussian detector errors

Table 3 Assessment of PMFD Accuracy Using RFSP Data at FPD 1000

Case			RFSP simulations		PMFD simulations		
zones	adjusters	type	Maximum Channel (kW)	Maximum Bundle (kW)	Maximum Channel (kW)	Maximum Bundle (kW)	Channel Power RMS Error
nominal	in	diff	7152	960	7325	1069	2.69
nominal	in	map			7245	993	1.42
nominal	in	err			7265	992	1.76
empty	in	diff	8512	1205	8633	1270	2.44
empty	in	map			8634	1246	1.27
empty	in	err			8633	1275	1.53
nominal	out	diff	9882	1395	10181	1509	2.48
nominal	out	map			10010	1470	1.27
nominal	out	err			10070	1457	1.68

note:
diff = Diffusion theory Only
map = Diffusion + mapping (no detector errors)
err = Map with 5% Gaussian detector errors

Table 4 Effect of Random Detector Errors on PMFD Performance Using RFSP Data at FPD 1000

Random Error	Max. Channel Power		Max. Bundle Power		Channel Power RMS Error
	Whole Core		Whole Core		
	(kW)	% Difference	(kW)	% Difference	
1	7359	2.9	995	3.6	1.79
2	7373	3.1	1010	5.2	1.64
3	7384	3.2	1023	6.6	2.03
4	7281	1.8	1006	4.8	1.65
5	7373	3.1	1010	5.2	2.15
6	7266	1.6	1013	5.5	2.11
7	7351	2.8	988	2.9	2.02
8	7189	0.5	1009	5.1	1.86
9	7241	1.2	992	3.3	1.99
10	7322	2.4	1033	7.6	2.26
11	7338	2.6	1021	6.4	2.16
12	7249	1.4	997	3.9	1.61
Average		2.2		5.0	1.94
No Error	7245	1.3	993	3.4	1.42

Notes:
σ for random error = 0.05
RFSP max. channel power = 7152 kW
RFSP max. bundle power = 960 kW

Table 5 Effect of Systemic Detector Errors on PMFD Performance Using RFSP Data at FPD 1000

Failed Assembly	Max. Channel Power		Max. Bundle Power		Channel Power RMS Error
	Whole Core		Whole Core		
	(kW)	% Difference	(kW)	% Difference	
VFD-8	7366	3.0	996	3.8	1.75
VFD-24	7349	2.8	1012	5.4	1.73
None	7359	2.9	995	3.6	1.79
All	7324	2.4	1069	11.3	2.66

Notes:
σ for random error = 0.05
RFSP max. channel power = 7152 kW
RFSP max. bundle power = 960 kW

Table 6 Effect of Random Irradiation Errors on PMFD Performance Using RFSP Data at FPD 1000

Irradiation Error	Max. Channel Power		Max. Bundle Power		Channel Power RMS Error
	(kW)	% Difference	(kW)	% Difference	Whole Core
1 Diffusion	7326	2.4	1068	11.3	2.79
2 Diffusion	7289	1.9	1081	12.6	2.63
3 Diffusion	7341	2.6	1073	11.8	2.61
Average (Diffusion)		2.3		11.9	2.68
1 Mapping	7234	1.1	993	3.4	1.46
2 Mapping	7230	1.1	995	3.6	1.43
3 Mapping	7252	1.4	997	3.9	1.43
Average (Mapping)		1.2		3.6	1.44
No Error	7245	1.3	993	3.4	1.42

Notes:
σ for random error = 0.01
RFSP max. channel power = 7152 kW
RFSP max. bundle power = 960 kW

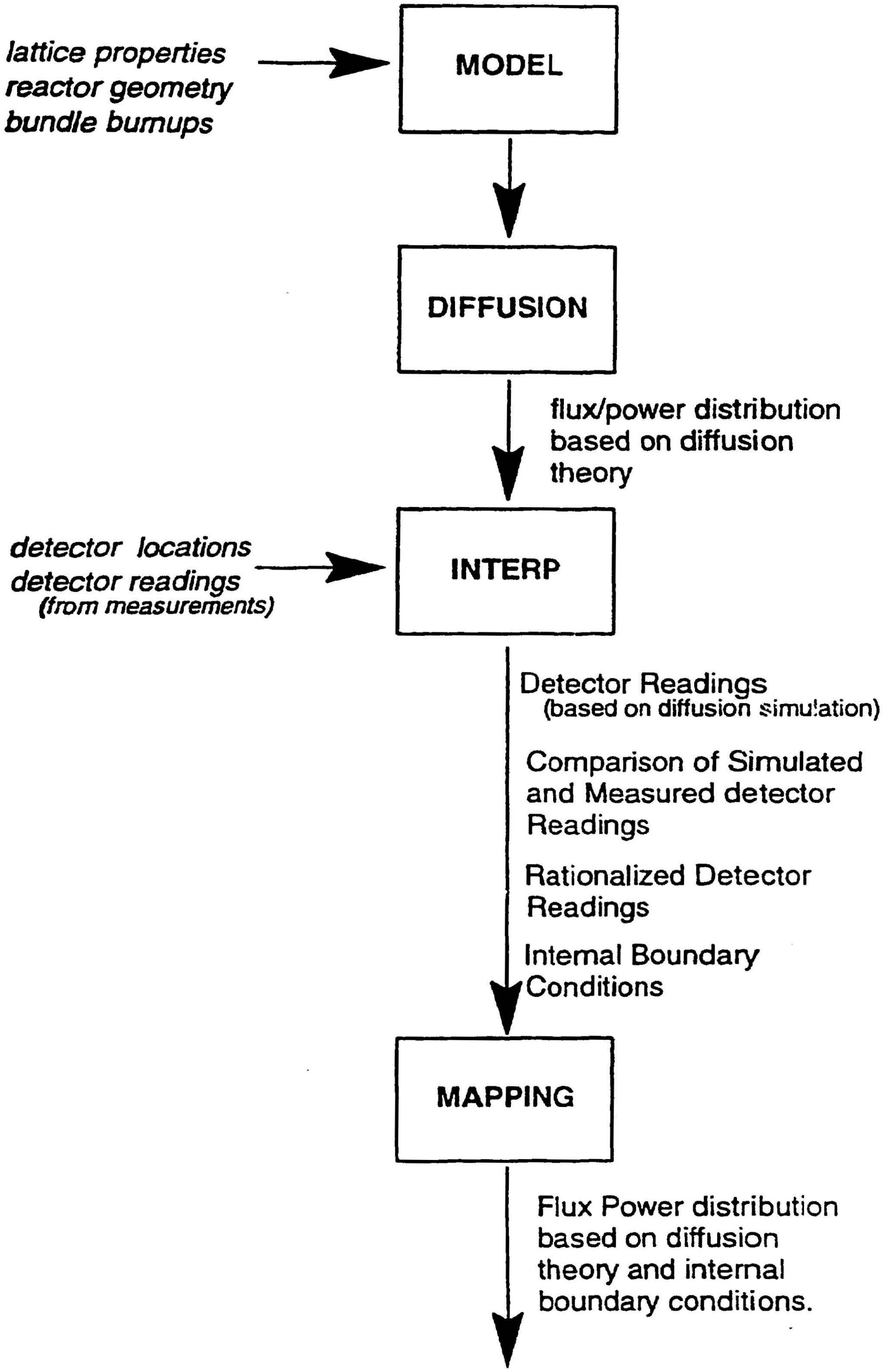

Figure 1 Flow Chart of PMFD

Figure 2 PMFD Diffusion vs. RFSP at FPD 1000

CHANNEL POWER ERRORS (1000=100%)

	1	2	3	4	5	6	7	8	9	10	11	12	13	14	15	16	17	18	19	20	21	22	23	24	25	28	27	28
AA										28	48	42	14	13	8	19	28	42	6									
A								-2	20	12	32	8	14	-1	6	2	5	12	-5	1	-15							
B								12	5	11	5	10	-4	2	-3	-6	-8	-7	-9	-11		-7						
C					23	14	8	5	10	-6	12	-10	2	-8	-3	-13	-14	-16	-18	-6	-2	3	18	21				
D				25	15	13	4	10	-1	4	-5	-5	-11	-9	-9	-16	-12	-28	-8	-13	5	3	21	13	30			
E				8	23		12	4	6	-5		-19	-5	-9	-12	-13	-15	-15	-11	-1	-1	13	15	29	7			
F			4	24	8	12	1	10	1	3	-7	-12	-10	-5	-8	-8	-3	-11		-2	14	5	29	13	30	7		
G		-5	10	7	15	-1	15	2	17	3	11	-4	-2	-1	-2	2	2	15	3	13	6	23	11	35	10	16	-2	
H		-9	2	12	2	10	2	21	14	32	24	24	4	1	6	5	28	26	27	12	25	13	31	20	34	4	5	
I	38	7	23	13	24	5	19	10	32	25	50	25	20	2	-3	10	24	33	23	27	14	32	26	50	27	33	17	40
J	36	21	11	28	10	17	9	25	16	39	32	41	13	-3			20	23	23	20	27	22	46	34	50	24	39	40
K	31	13	16	15	22	2	20	8	32	19	47	21	19	-3	-12	-1	6	18	11	23	15	35	34	51	32	49	24	50
L	14	14	6	15	1	11	7	18	11	33	13	39	3	-9	-13	-7	-1		7	7	28	20	54	30	59	20	48	18
M	10	3	10	1	7	2	13	2	19	8	27	6	13	-9	-25	-5	-15	-1	-4	14	13	37	35	58	37	52	21	34
N	8	6	9	17	10	14		11		16	3	12	2	-17	-15	-18	-12	-18	3	1	24	21	59	50	75	29	45	18
O	9	13	6	19	15	4	5	2	9	9	18	4	8	-7	-25	-1	-19	1	-3	14	11	39	36	77	48	56	23	42
P	20	12	-1	10				5	8	20	29	27	9	-11	-11	-4	12	7	18	6	27	14	54	42	66	26	47	31
Q	19	7	-9	-2	-11	-7	-8	-2	14	17	34	21	6	2	-14	9	6	25	10	16	8	25	29	50	25	49	19	51
R	16	-13	-13	-23	-23	-23	-12	-9	6	6	25	7	5	-12	-6	-8	7	2	7	-4	12	4	31	13	34	11	28	25
S		-40	-25	-25	-32	-25	-22	-9	-16	-4	-4	-4	-22	-13	-24	-16	-8	-10	-12	-3	-8	6	5	22	-6	22	-18	
T		-36	-17	-24	-16	-24	-24	-27	-19	-31	-17	-33	-31	-34	-27	-34	-18	-31	-18	-25	-3	-15	18		21	-8	9	
U			-24	-19	-20	-20	-33	-29	-37	-35	-50	-40	-58	-38	-45	-45	-39	-40	-42	-20	-25	-8	-8	17	-4	17		
V				-33	-15	-28	-27	-42	-37	-54	-61	-65	-62	-57	-48	-60	-48	-64	-41	-42	-14	-26	-1	-5	7			
W				-17	-24	-22	-35	-40	-47	-54	-68	-69	-74	-53	-61	-50	-66	-59	-57	-31	-37	-11	-22	9	-3			
X					-24	-15	-41	-46	-44	-52	-65	-63	-64	-57	-49	-61	-43	-69	-36	-51	-21	-33		-9				
Y							-47	-44	-42	-46	-42	-46	-58	-49	-51	-42	-45	-35	-48	-30	-42	-19						
Z								-56	-39	-40	-32	-43	-44	-52	-39	-46	-29	-37	-28	-39	-40							
ZZ										-37	-11	-25	-42	-40	-41	-29	-29	-3	-38									

Maximum of: 77 @ O-24

CORE-AVERAGED RMS ERROR = 2.69 %

Figure 3 PMFD Mapping (without Detector Error) vs. RFSP at FPD 1000

CHANNEL POWER ERRORS (1000•100%)

	1	2	3	4	5	6	7	8	9	10	11	12	13	14	15	16	17	18	19	20	21	22	23	24	25	26	27	28
AA										30	53	42	16	11	10	21	34	49	14									
A									22	17	35	13	12	-2	2	5	11	21	2	7	-12							
B							-2	11	10	16	12	12	-2	-8	-8	-5	1	3		-4		-12						
C					10	7	1	4	12		15	-2	2	-12	-12	-8	-2	-5	-9	-2	-4	-7	4					
D				9	2	-1	-2	4	-1	4		-2	-6	-11	-9	-12	-4	-21	-7	-13	-4	-9	-2	-9	2			
E				-6	-1	-16		-1	1	-4		-14	-5	-9	-12	-11	-9	-13	-11	-9	-12	-8	-11	-7	-18			
F			-6	6	-8	-9	-8		-2		-6	-11	-11	-7	-11	-7	-2	-9	-5	-9	-4	-13	-7	-16	-4	-15		
G		-9	-3	-4	-2	-13		-7	7	-2	5	-8	-8	-7	-5	-3		6	-4	-3	-10	-5	-12		-15	-14	-20	
H		-11	-3	-3	-13	-10	-12	5	3	20	15	15	-3	-2	-3	1	15	17	9		-2	-12	-8	-9	-2	-16	-17	
I	46	15	16	1		-18	-1	-5	15	11	39	14	14	-11	-6	-2	16	16	7		-9	-8	-13		-1	3	11	37
J	49	27	9	13	-10	-9	-8	7		24	21	33	1	-7	-15	-4	5	12			-7	-10	-6	-7	9	5	22	38
K	39	19	10	5	2	-14	1	-5	18	7	39	12	15	-14	-14	-13		1	-2	-5	-9	-6	-3	1	1	16	12	33
L	26	19	6	5	-13	-7	-7	3		24	6	15	-3	-8	-21	-6	-12	-4	-13	-10	-6	-11	4	-6	16		25	12
M	26	17	11	-5	-13	-17	-1	-8	9	1	21	3	16	-14	-17	-11	-11	-10	-12	-10	-9	-6	-7	1	8	20	17	22
N	28	21	13	11	-6	-5	-11	1	-6	11		12		-9	-19	-12	-16	-17	-12	-11	-8	-8	1	8	32	12	28	19
O	29	29	13	18	6	-4	-2	-2	5	7	18	3	12	-11	-20	-6	-16	-7	-9	-7	-6	-1	1	27	23	26	18	31
P	46	35	8	11	-3	-4	-2	4	8	22	30	30	7	-8	-16		7	7	5	-2		-8	8	11	29	15	35	37
Q	46	30	1	1	-14	-11	-7		18	20	41	24	11	-5	-16	6	11	21	9		-1	-7	1	3	5	23	21	45
R	37	3	-1	-17	-23	-24	-8	-1	13	16	34	18	9	-11	-11		11	11	2	-4	-5	-8	-8	-9		1	10	25
S		-21	-12	-15	-24	-16	-11	2	-1	9	12	8	-6	-5	-10	-7	7	-2	-1	-7	-7	-11	-2	-6	-17	-2	-24	
T		-20	-4	-11	-1	-7	-8	-6	1	-4	6	-5	-10	-10	-9	-10		-7	-7	-10	-6	-12	3		-1	-15	-10	
U			-10	-6	-8	-6	-10	-5	-4	-2	-9	-4	-22	-11	-12	-18	-2	-12	-13	-6	-9	-11	-5	-1	-8	-3		
V				-19	-4	-14	-3	-10	-3	-11	-18	-17	-24	-18	-17	-20	-12	-22	-15	-13	-4	-11	-14	-6	-9			
W					-5		-5	-7	-5	-10	-17	-20	-24	-16	-19	-12	-17	-22	-17	-7	-11	-5	-11	1	-1			
X						13	-8	-4	1	2	-12	-6	-18	-16	-16	-14		-18		-11		-9	4					
Y							-7	-2	10	5	12	5	-9	-15	-10	-3	5	6		4	-7	-2						
Z								-8	8	13	17	8		-7	-2		11	9	10	2	-10							
ZZ										11	39	21	6	1	4	10	16	36	7									

Maximum of: 53 @ AA-11

CORE-AVERAGED RMS ERROR = 1.42 %

Figure 4 PMFD Mapping (with Detector Error) vs. RFSP at FPD 1000

CHANNEL POWER ERRORS (1000-100%)

	1	2	3	4	5	6	7	8	9	10	11	12	13	14	15	16	17	18	19	20	21	22	23	24	25	26	27	28
AA										27	57	37	22		11	5	31	38	15									
A								-1	16	21	33	21	5	1	-13	3	-6	17	-1	15	-3							
B							-5	4	8	10	24	15	6	-26	-5	-25	-9	-16	6	3	12	4						
C					2	2	-5	2	3	1	18	10	-2	-5	-32	-10	-25	-14	-8	9	9	8	31	23				
D					-6	-10	-5	-2	-2	1	8		1	-19	-7	-21	-4	-25	-4	-6	6	15	20	26	27			
E				-16	-18	-26	-3	-3	-5	-2	8	-1	-5	-5	-18	-9	-4	-6	-11	-10	3	9	34	23	17			
F			-13	-3	-21	-20	-8	-5	-6	-5	3	-6	-8	-11	-12	-10	2	-2	-9	-5	2	13	23	29	15	9		
G		-11	-6	-11	-7	-18	-8	-14		-7	-2	-12	-13	-12	-12	-10	-4		-3	-3	1	5	15	16	5	-7	-11	
H		-10	-6	-10	-23	-22	-25	-5	-3	10	-2	-5	-15	-12	-14	-8	-5	6	3	5			-2	4		-10	-24	
I	55	21	14	-6	-12	-41	-26	-17	10	5	20	-3	1	-25	-17	-17	3	-2	11	3	-1	-6	-8	-3	2	-3		17
J	58	33	7	4	-27	-32	-32	-5	-3	22	13	24	-6	-16	-27	-13	-8	8		7	-6	-3	-10	-5	3	2	4	21
K	81	21	4	-1	-14	-32	-16	-16	10	4	36	11	13	-19	-19	-20	-4	-5	-2	-7	-5	-6	2		6	9	6	20
L	30	15	5	-6	-24	-25	-21	-8	-5	21	10	42	2	-6	-23	-10	-17	-9	-19	-11	-7	-5	7	1	16	1	19	7
M	21	19	2	-10	-29	-32	-22	-17		1	32	25	34	-7	-15	-12	-16	-15	-22	-20	-7	-2	5	8	15	20	16	16
N	32	14	14		-12	-25	-23	-10	-9	9	13	34	20	-3	-12	-13	-17	-22	-22	-17	-7	1	12	22	39	18	26	18
O	17	29	2	20	-1	-2	-14	-4		10	23	17	24	2	-14		-16	-7	-11	-6		10	18	42	36	33	23	32
P	40	16	9	2	4	-12	-2	-4	8	17	36	37	22	3		4	13	8	9	2	11	11	31	32	43	26	41	42
Q	28	27	-8	9	-24	-1	-17		7	18	38	33	20	22	1	19	12	24	12	9	9	14	33	30	23	35	29	52
R	36	-4	4	-21	-9	-30	-1	-7	10	5	35	17	22	4	14	2	12	6	7		6	6	16	15	18	12	20	32
S		-18	-11	-4	-19	-5	-9	6	-4	10	7	11	-5	6	-7	-3		-7	-5	-4	-3		5	7	-9	9	-17	
T		-14	6	1	11	8	1		5	-6	6	-9	-8	-13	-8	-17	-9	-19	-13	-16	-2	-11	7	-8	7	-11		
U			6	8	24	9	7	3	1		-15	-7	-29	-14	-22	-27	-21	-32	-28	-13	-13		-14	3	-12	6		
V				7	14	21	8	3	2	-10	-21	-24	-28	-30	-26	-33	-31	-42	-28	-25	-2	-8	2	-13				
W				17	22	14	16	3	6	-5	-19	-18	-30	-28	-39	-17	-24	-31	-28	-10	-17	2	-13	11	-3			
X					16	37	5	12	16	13	-15	-12	-25	-51	-43	-27	1	-26	-1	-17	2	-12	11	-1				
Y							11	10	27	15	6	-3	-29	-46	-49	-17	-5	3	-8	4	-12	1						
Z								6	17	17	14	-2	-15	-34	-22	-21	2		7	-4	-10							
ZZ										13	35	12	-10	-15	-18	-3	1	30	-2									

Maximum of: 58 @ J- 1

CORE-AVERAGED RMS ERROR = 1.76 %

Figure 5 : Comparison of PMFD and RFSP Channel Powers in Row M at FPD 1000

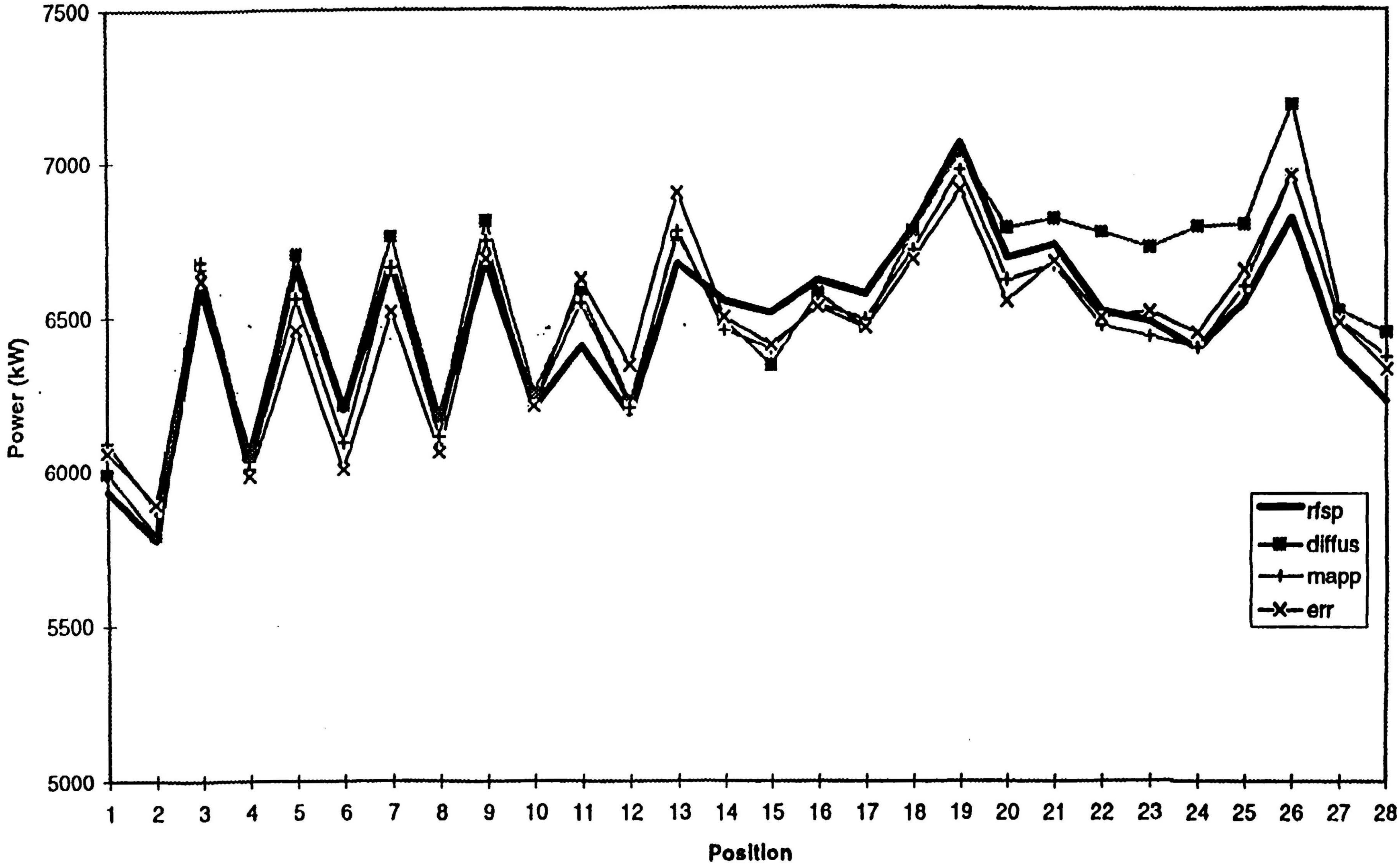

Figure 6 : Comparison of PMFD and RFSP Bundle Powers in Channel M-14 at FPD 1000